



UNIVERSITÀ  
DEGLI STUDI  
FIRENZE

# FLORE

## Repository istituzionale dell'Università degli Studi di Firenze

### **Influence of car front-end designs on motorcyclists' trajectory in head-on and side-on-head crashes**

Questa è la Versione finale referata (Post print/Accepted manuscript) della seguente pubblicazione:

*Original Citation:*

Influence of car front-end designs on motorcyclists' trajectory in head-on and side-on-head crashes /  
Alberto Perticone;  
Valerio Nardomarinò;  
Niccolo Baldanzini;. - In: IOP CONFERENCE SERIES: MATERIALS SCIENCE AND ENGINEERING. - ISSN 1757-

*Availability:*

The webpage <https://hdl.handle.net/2158/1356881> of the repository was last updated on 2024-04-21T16:25:45Z

*Terms of use:*

Open Access

La pubblicazione è resa disponibile sotto le norme e i termini della licenza di deposito, secondo quanto stabilito dalla Policy per l'accesso aperto dell'Università degli Studi di Firenze (<https://www.sba.unifi.it/upload/policy-oa-2016-1.pdf>)

*Publisher copyright claim:*

La data sopra indicata si riferisce all'ultimo aggiornamento della scheda del Repository FloRe - The above-mentioned date refers to the last update of the record in the Institutional Repository FloRe

(Article begins on next page)

# Influence of car front-end designs on motorcyclists' trajectory in head-on and side-on-head crashes

A Perticone<sup>1</sup>, V Nardommarino<sup>1</sup>, N Baldanzini<sup>1</sup>

<sup>1</sup> Department of Industrial Engineering, University of Florence, Via di Santa Marta 3, 50139 Firenze, Italy

E-mail: [alberto.perticone@unifi.it](mailto:alberto.perticone@unifi.it)

**Abstract.** Motorcyclists are highly vulnerable road users, and cars are one of their primary crash opponents. This study investigates the influence of car front-end designs on motorcyclist trajectory in head-on and side-on-head crashes. The analysis is based on a dataset of 120 multi-body crash simulations conducted using MADYMO and post-processed with MATLAB. An analysis of 1412 real-world Powered Two-Wheeler (PTW) to car accidents was conducted to determine the most common crash configurations and the associated ranges of the variables, such as vehicle speeds and contact points. Three PTW styles (sport-touring, scooter, and sport) and four car front-end designs (Sport utility vehicle (SUV), Family Car/Sedan (FCR), Roadster (RDS), and Multi-purpose vehicle (MPV)) were considered.

The study examined the riders' thrown distance in both collision types. It was observed that, regardless of the collision type, the head was identified overall as the primary body region coming into contact with the opposing vehicle, followed by the chest and neck. In frontal collisions, an augmented bonnet height corresponded to an increased incidence of head contact, whereas a lower bonnet height resulted in a higher frequency of chest contact. Moreover, the thrown distance depended also on PTW speed, particularly for sport and sport-touring motorcycles. Notably, contact with the car windscreen was only observed at velocities exceeding 60 km/h, whereas impact with the bonnet leading edge occurred exclusively below this threshold. Due to the shielding effect of their PTW's fairing, scooter riders predominantly experienced no contact with the opposing vehicle. Sport-touring motorcycles exhibited a more vertical trajectory upon ejection, leading to a greater likelihood of overturning and subsequent rearward head impact with the vehicle. In contrast, sport motorcycles tended to forward projections with a high likelihood of chest contact. In the case of lateral impacts, it was observed that vehicles with a more prominent profile, such as SUVs and MPVs, equipped with protruding bumpers, effectively restrained riders. In this case, vehicle speed did not exert a significant influence on the thrown distance. Additionally, the presence of a conspicuous fuel tank and the initial posture of the rider on the PTW played a crucial role in determining the final thrown distance. Due to their upright postures and the absence of a pronounced fuel tank, scooter dummies were thrown further than others, thus causing head contact with the windscreen.

These findings highlight the importance of car front-end design and PTW fairings in mitigating riders' injuries and provide valuable insights to vehicle manufacturers for developing tailored safety measures for riders.

## 1 Introduction

Motorcyclists represent a significant group of road users whose safety is of paramount concern due to their inherent vulnerability on the road. The exposure to potential risks and the limited protection available on their Powered-Two-Wheelers (PTWs) make riders particularly vulnerable in accidents. Statistics concerning riders' fatalities and injuries in Europe underscore the urgent need for adequate safety measures and motorcycle consumer rating programs [1].

Although road deaths in 2021 fell by 10% (2,000 fatalities) compared with pre-pandemic 2019, in 2022, fatalities rose by 3% to the previous year [2]. Furthermore, the share differs greatly among road users, with vulnerable road users (pedestrians, cyclists, and PTW riders) representing almost 70% of total fatalities [2]. The road safety context is also different across Europe, and it is recognized the significance of tailored approaches to address the vulnerabilities faced by motorcyclists in each country. In this regard, Italy and France still had the highest number of rider fatalities in 2020, even though this number has decreased more than the EU average over the past decade [3]. In addition to fatalities, non-fatal injuries among motorcyclists also present a concerning picture. In 2018, the EU set a 50% reduction target by 2030 for road deaths and, for the first time, also for serious injuries. This objective was defined in the Commission's Strategic Action Plan on Road Safety and EU road safety policy framework 2021-2030 [4], which also lays out road safety plans aiming to reach zero road deaths by 2050 within the "Vision Zero" program. Serious injuries can lead to long-term disabilities, medical costs, and a diminished quality of life for affected individuals. As evidenced by the statistical data, motorcyclists are indeed vulnerable road users (VRUs) in Europe, facing a disproportionately high risk of fatalities and injuries compared to that faced by other road users such as car drivers.

Addressing this issue necessitates understanding accident events in detail, as well as the injuries and their causes to develop countermeasures for the protection of PTW riders. In this regard, it is already known that impact speed [5–7], impact angle [8,9], impact location [10,11] and PTW style [1,12–15] have great influences on the riders' risk of injuries. The present study wants to answer the research question of the car front-end design influence on the motorcyclists' trajectory during the two most representative types of crashes: head-on and side-on-head. Similar studies on the influence of vehicle shapes and stiffnesses have been common in recent years for pedestrian and cyclist safety, but the research efforts on PTW users were scarce. It was demonstrated that bicyclists are exposed to lower impact speed and are less frequently and severely injured than pedestrians, with longer head contact time and shorter longitudinal throws [16]. Furthermore, it was shown that the geometry of the car largely determines the contact points of the different body regions with the bonnet [17] and that vehicles with a high bonnet leading edge are likely to cause higher head ground contact speeds at 30 km/h [18], and consequently, low-fronted cars provide better containment of the pedestrian on the bonnet. SUVs and vans appear to be more aggressive for head-ground contacts, while at 40 km/h, a low front might not give any benefit in reducing the severity of head-ground impacts. Later, relationships between passenger car front shape and pedestrian injury risk derived from accident data were quantified, showing that the bumper geometry is statistically significant for AIS2+ leg injury risk and femur/pelvis injury occurrences [19]. On

the other hand, the authors concluded that the passenger car front shape did not show statistical significance for AIS3+ thorax and head injuries and, in general, the passenger car front shape parameters were less influential than impact speed and pedestrian age for pedestrian injury risk. Recently, a couple of papers have been published about the influence of vehicle front-end design on the head injury risk of motorcyclists (Xiao et al., 2022, 2020), demonstrating that the bonnet length has high influences on motorcyclist head injuries and that one-box vehicles can be more likely to cause head injuries than the other four vehicle types: i.e., Sedan, MPV, SUV, and EV (Electric Vehicle). The authors also noted that the effects of vehicle shape parameters on motorcyclist and pedestrian head injuries are quite different and the trend of decreasing the bonnet angle and increasing the bonnet length can potentially reduce the head injury risk of motorcyclists.

To answer the research question, the present study investigates the effect of four car front-end designs on the riders' thrown distance in two collision types, i.e., head-on and side-on-head, in conjunction with three different PTW styles: sport-touring, scooter, and sport.

## 2 Method

### 2.1 Data collection

Configurations and speed ranges were defined based on a dataset of 1412 real PTW-to-car accidents collected from ISO 13232, MAIDS, and GIDAS databases. The dataset included only accidents involving L3 vehicles, i.e., PTWs with a maximum design speed exceeding 45 km/h and an engine capacity exceeding 50 cm<sup>3</sup>. The dataset exclusively consisted of accidents with a two-wheeled motor vehicle (MC) without a pillion rider and rider seated on an upright motorcycle at the time of impact. The dataset was sorted to identify the most representative crash configurations coded with the three-digit system provided by ISO 13232. The code identifies the contact points (CPs) and relative heading angle (RHA) between MC and opposite vehicle (OV), based on the following coding scheme: the first two digits of the code indicate the CPs of the OV and MC, respectively, while the third digit corresponds to the RHA between the two vehicles; seven contact points are identified for the OV in a clockwise direction, starting from the center line of the frontal bumper (CP=1) and ending at the center line of the rear bumper (CP=7); for the MC, the first contact point (CP=1) represents the front wheel, the third contact point (CP=3) represents the rear wheel, and the second and fourth contact points (CP=2,4) indicate the left and right sides of the MC, respectively; the third digit in the code is the multiple 1 to 8 of a 45-degree range that returns the RHA measured clockwise from the front.

The 1412 collected accidents were sorted according to occurrence frequency (Figure 2.1). Since this study was devoted to evaluating the influence of car front-end designs, head-on-side (42%), head-on-rear (9%), and rear-end (4%) accidents were not considered. Configurations 114, 115, and 143 were investigated, representing head-on (21%) and side-on-head accidents (10%), respectively. The data was used to define the conditions for the simulations.

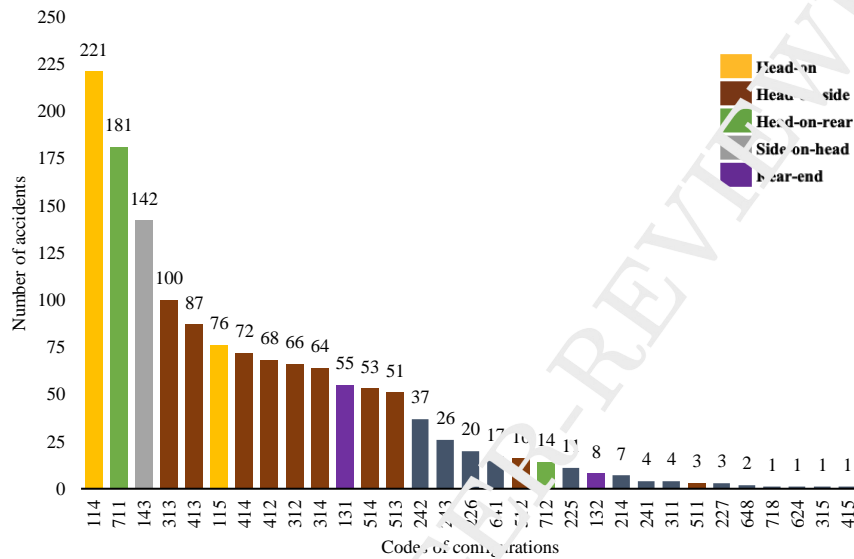


Figure 2.1 – Crash configuration distributions across data collected from ISO 13232, MAIDS, and GIDAS.

## 2.2 Simulation set-up

For the head-on crashes, the OV was chosen to be stationary since it is crucial to emphasize that this study focuses exclusively on evaluating trajectories rather than injuries. Specifically, the assessment considers trajectories within a reference system integral to one of the two vehicles, namely the OV, in this study. Consequently, the cinematic characteristics of the system, unaffected by the forces generating it, remain consistent for a given relative speed, regardless of which vehicle possesses a higher speed or greater mass. Thus, under fixed relative speed conditions, the accelerations measured by the dummy or the OV are identical, irrespective of whether the speed is ascribed to the heavier or lighter vehicle. However, it is essential to note that when considering an external reference system and accounting for injury assessment, discrepancies in speed attribution yield divergent outcomes. The speed of the MC was defined between 30 and 90 km/h with five steps of 15 km/h each. Even though the original dataset reported the range for the MC down to 0 km/h in “114” and “115” accidents, 30 km/h was considered the minimum significant speed of the MC to appreciate a thrown trajectory since no ejections were noticed by simulating a few sample configurations below this threshold with the OV stationary. Conversely, the MC was kept stationary for the side-on-head crashes to maximize the chance that the PTW rider could hit the OV, and the OV speed range was defined between 30 km/h and 90 km/h, with increments of 15 km/h, for uniformity with the other crash type although its maximum speed across the databases was 65 km/h. The simulations were set up in MADYMO and performed with version 2020.2. A total of 120 simulations were run, considering the five speeds, three PTWs, four OV profiles, and two collision types. The RHA between the two vehicles was maintained at its nominal value, i.e., 180 degrees in the first collision type and 90° in the second one. This study did not consider angled crashes, and their effect on dummy trajectories was not evaluated. Every parameter (speed, angle, OV type, MC type) was managed by HyperStudy to automatically generate the simulation files with a run-time of 500 ms. As this study only evaluated primary impacts, a 500 ms window was considered adequate to capture these events in agreement with other studies [23–29]. The coefficient of friction between the dummy and the car was demonstrated to have a remarkable effect on trajectories and head impact time and was therefore set to 0.3, which is in accordance with

several studies [6,18,20,30,31]. A friction coefficient of 0.8 was assumed for the tire-ground contact to represent a dry asphalt road [32–34].

The thrown trajectories were recorded until the first interaction between the rider's head and the OV. The visual representation of the trajectories is provided in Appendix A (Figure A.2, Figure A.3, Figure A.4, Figure A.5). Shaded stickmen represented the riders in their initial positions on the PTWs, excluded from the visual representation; the solid colors indicated their final position when the acquisition stopped.

### 2.3 Vehicle models

Three vehicles, representative of three PTW styles, and four front-end designs of car models were used in this study. The three PTWs were developed during previous research at the University of Florence and were already used in multi-body crash simulations [35,36]. The computer-model fleet comprehended a sport-touring, a sport, and a scooter style PTWs, Figure 2.2, and four Generic Vehicles (GVs) for cars, Figure 2.3 (left). GV models are generic replications of current car fronts. The car fronts were developed within the TB024 EuroNCAP Protocol [37] for kinematic comparisons only and should not be used for evaluations of injury metrics as they do not meet the UN-R127 requirements. The GV models represented Sport Utility Vehicle (SUV), Family Car/Sedan (FCR), Roadster (RDS), and Multi-Purpose Vehicles and Superminis (MPV). In a previous study [20], three-dimensional median geometries were used to obtain representative vehicle shapes. The four FE models retrieved from that work, Figure 2.3 (left), were converted in MADYMO as facet surfaces and contact characteristics, Figure 2.4, were attributed to the five main front-end sub-groups: roof/windscreen, bonnet, bonnet leading edge (BLE), bumper, and spoiler, Figure 2.3 (right). These contact characteristics were obtained numerically by propelling a rigid cylindrical impactor against their FE counterparts in RADIOSS. The procedure was repeated at eight locations on the spoiler, bumper, bonnet lead, and bonnet at the vehicle centerline. The output curves (Figure 2.4) complied with the corridors supplied in the previous studies [20] to generate reasonable contact forces in the pedestrian-vehicle interaction study. However, they did not account for the stiffness out of the centerline of each car model since, in this study, all the simulated crashes were centered and ignored potential regions of localized stiffness along the centerline.

The vehicle curb weights were increased by 150 kg for the driver and front passenger as specified in the Euro NCAP pedestrian testing protocol for a total amount of: 1775 kg for the SUV, 1690 kg for FCR, 1590.5 kg for MPV, and 1462.5 kg for RDS. The vehicles have only one degree of freedom: the X-direction in the vehicle coordinate system. The global coordinate system was defined as shown in Figure 2.3: X-direction was the driving direction of the OV (longitudinal axis), and  $x=0$  at the foremost point of the vehicle at the beginning of the acquisition ( $t=0$ ). Negative values referred to the acquisition points in front of the OV when the riders were still on their PTW. Y-direction was the lateral vehicle axis with  $y=0$  at the vehicle centerline, whereas Z-direction was vertical and upwards with  $z=0$  at the ground level.

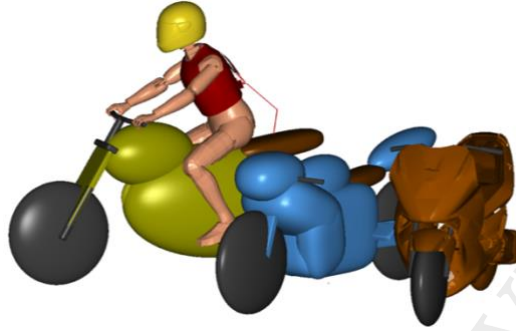


Figure 2.2 - PTW fleet, helmeted rider dummy, and BSJ.

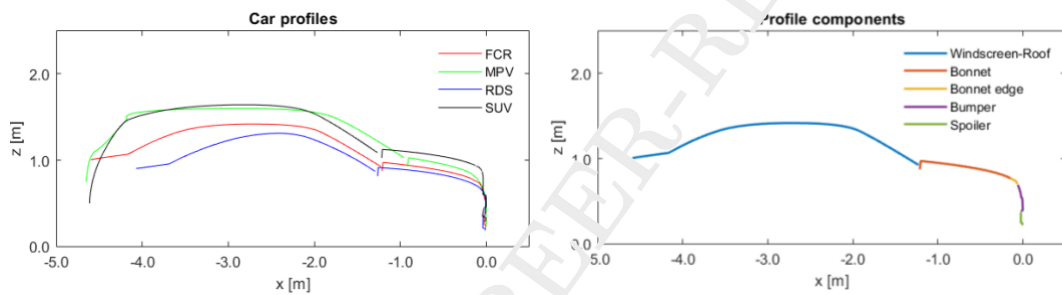


Figure 2.3 - The four OV profiles (left) and the five parts of the front-end design (right).

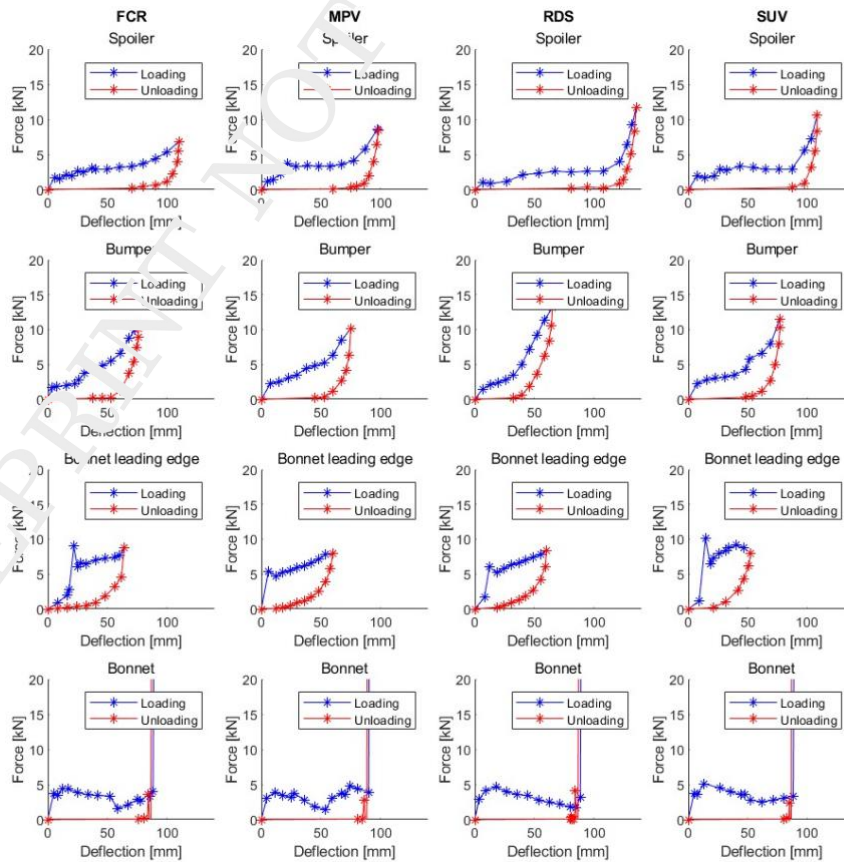


Figure 2.4 - Contact characteristics per parts and OV type included in the multibody models.

The Motorcycle Anthropometric Test Dummy (MATD) used in this study is based on the Hybrid III Anthropometric Test Dummy design, and it was specifically developed to model riders. The MATD was fitted with a helmet, and a state of equilibrium was achieved for the entire model by applying a gravitational load to the dummy and the PTW (e.g., pre-compressed suspensions). It is important to note that a rider's sitting position can vary significantly, and it is influenced by numerous factors, including human factors (such as physical characteristics, riding experience, duration of riding, cognitive load), motorcycle design characteristics, and environmental variables (such as road conditions, weather, and traffic conditions) [38]. When comparing the actual comfortable position of a real rider with the anthropometric measurements of the MATD, several disparities were observed [39]. Hence, the positioning of the dummy was carried out following the recommended procedures outlined by ISO [40], and the joint angles were extrapolated from relevant literature to achieve a natural ergonomic posture that corresponds to the optimal riding position [41].

### 3 Results

The results are categorized into frontal and lateral crashes, Figure A.1. Each collision type was subjected to a comprehensive analysis of two influential parameters: the style of the PTW and the type of front-end design. The output under control was the trajectory of the head, henceforth denoted in figures as "Distance," which represented the thrown distance along the X-axis measured at the head's center of gravity in the reference system described in section 2.3.

#### 3.1 Frontal Crash

In frontal crashes, the thrown distance of the dummy increased with a magnitude dependent on speed for both the PTW styles and the OV front-end designs, Figure 3.1. Every collision causing head contact was plotted in the chart, identifying the car part involved. A trendline minimizing the sum of squares of a power function was drawn for each PTW, Figure 3.1 (left), and car profile, Figure 3.1 (right). Every line showed a clear dependence on the closing speed, primarily upon different PTW styles: the sport PTW had the highest slope and vertical shift, while the scooter reported the lowest values, with a weak dependence on speed. The sport-touring showed intermediate values of slope and vertical shift. With reference to car profiles, the dependence on speed was more accentuated for RDS and less for FCR. Similar behaviors were noticed for SUV and MPV. It was worth noting that contacts on the windscreen happened only at and above 60 km/h, whereas those on the bonnet edge were only below 60 km/h. Contacts on the bonnet were largely spread across the whole speed span.



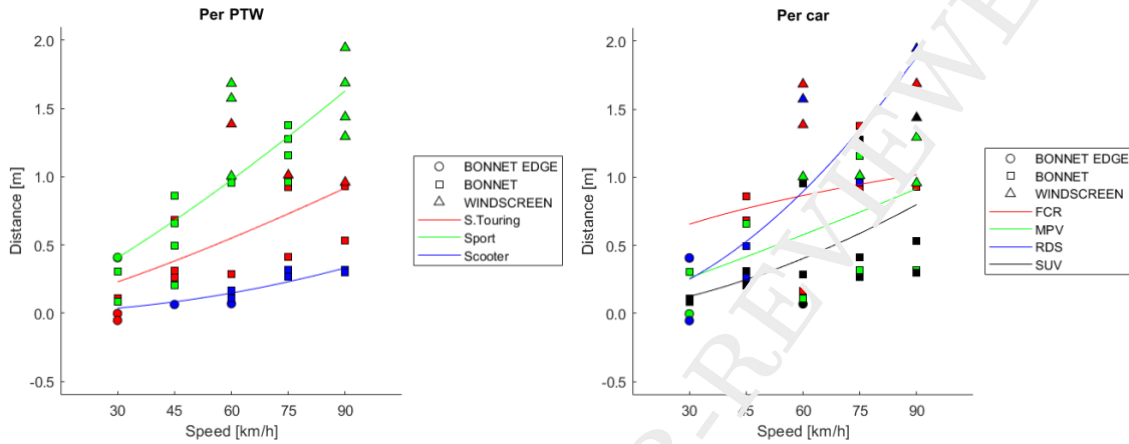


Figure 3.1 - Influence of speed in frontal crash per PTW (left) and per car (right). Every collision causing head contact was plotted in the scatter with a geometric symbol and a trendline was drawn over this data.

### 3.1.1 Influence of PTW

The boxplot analysis, Figure 3.2, and ANOVA tests confirmed that the scooter ( $M=0.27$  m,  $SD=0.106$  m) had the shortest thrown distance among the PTWs, significantly different ( $p$ -value  $< 0.01$ ) from that of the other styles. Also, the sport ( $M=0.98$  m,  $SD=0.550$  m) and the sport-touring ( $M=0.41$  m,  $SD=0.425$  m) differed significantly from one another ( $p$ -value  $< 0.01$ ). The total number of all the speed pairs per PTW was 20, but each boxplot did not count for the same number of simulations due to the presence of some no-contact instances ( $N_{S.Touring}=15$ ;  $N_{Sport}=20$ ;  $N_{Scooter}=10$ ).

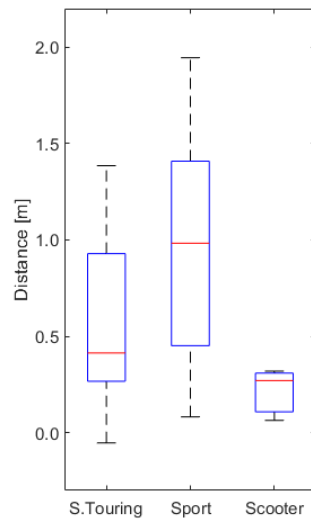


Figure 3.2 - Collision distance per PTW in frontal crashes.

A further investigation interested the contact points during the crash. The distribution per car parts, Figure 3.3 (left), showed that between 50% and 75% of the collisions involved the three PTWs with direct contact between the dummy and the car bonnet or bonnet leading edge. Other contacts involved the windscreen or even no contact at all, in the case of scooter and sport-touring. However, a Chi-squared test with the null hypothesis that one car part is independent of an assigned PTW style could not be rejected on a 5% significance level for any PTW style,

Figure A.6 (a). Based on the distribution per dummy's body regions, Figure 2.3 (right), the sport PTW dummy consistently came into contact with the OV's, with a notable occurrence of chest contacts (40%), which was deemed significantly related to the type of PTW by the Chi-squared test, Figure A.6 (b). On the other hand, sport-touring motorcycles and scooters exhibited instances where no contact with the OV was observed in 25% and 50% of cases, respectively, and the sport-touring motorcycle dummy experienced the highest head contact percentage (75%). Notably, the no-contact instances, despite not being below the 5% significance level, Figure A.6 (b), showed a marked variability in the PTW style.

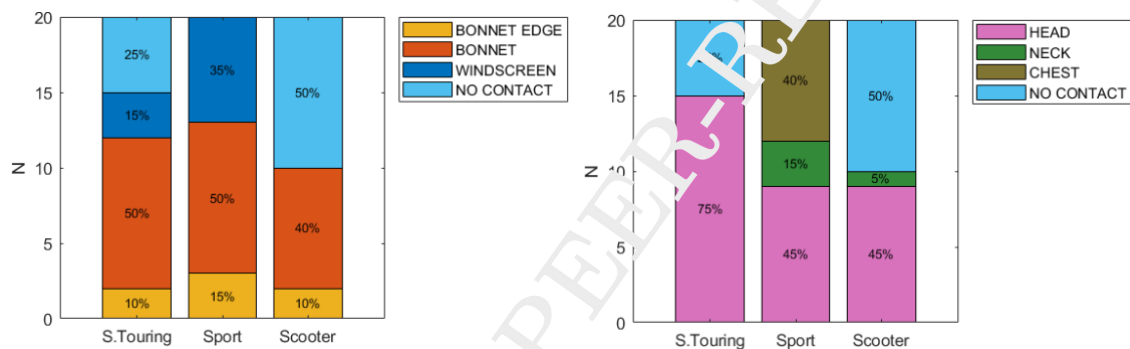


Figure 3.3 - Contact points per car parts (left) and dummy's body regions (right) across PTWs in frontal crashes.

### 3.1.2 Influence of car profile

The boxplot analysis and ANOVA tests confirmed that the SUV ( $M=0.29$  m,  $SD=0.450$  m) had the lowest thrown distance among the OV's, significantly different ( $p\text{-value} < 0.01$ ) from that of the other car profiles, Figure 3.4. FCR scored higher values ( $M=0.89$  m,  $SD=0.546$  m), while MPV ( $M=0.49$  m,  $SD=0.446$  m) and RDS ( $M=0.49$  m,  $SD=0.730$  m) reported similar median values, with wider variance for the latter. Each boxplot did not count for the same number of simulations ( $N=15$ ) due to the presence of some no-contact instances ( $N_{FCR}=12$ ;  $N_{RDS}=7$ ;  $N_{MPV}=12$ ;  $N_{SUV}=14$ ).

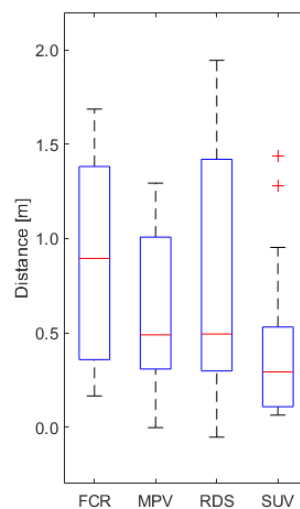


Figure 3.4 - Collision distance per car profile in frontal crashes.

The FCR and RDS exhibited an equal percentage of chest contacts (20%), Figure 3.5 (right). Notably, the SUV demonstrated the highest frequency of contact with the dummy, with the lowest occurrence of no-contact instances and contacts on the windscreen, both at 7%, Figure 3.5 (left). Most of the contacts with the SUV involved the head on the bonnet. In contrast, approximately half of the collisions involving the RDS did not directly result in contact (53%), while a moderate percentage (20%) of contacts occurred on the chest (a value shared with the FCR). Contacts on the head were the lowest reported (27%), as illustrated in Figure 3.5 (right). Eventually, the MPV exhibited the highest number of contacts on the windscreen (27%). From the Chi-squared tests, neither body regions nor car parts could reject the null hypothesis of independence from the front-end designs with a 5% significance level, Figure A.6 (a)-(b).

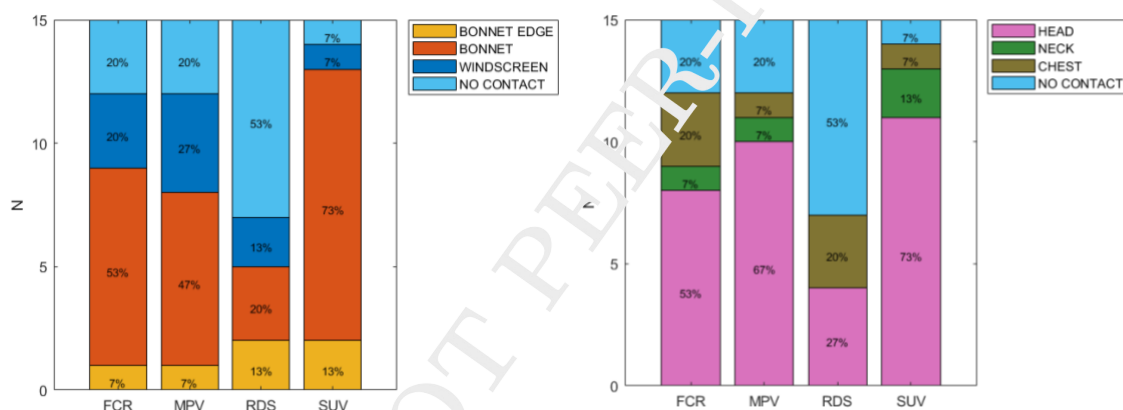


Figure 3.5 - Contact points per car part (left) and dummy's body regions (right) across OV's in frontal crashes.

### 3.2 Lateral Crash

In this case, the scooter reported the longest distance, the sport style the shortest, and the sport-touring maintained its central position between the other two, Figure 3.6 (left). Only the scooter showed a moderate positive derivative between 30 and 90 km/h. Grouping the results per car profile, FCR and RDS performed similarly, with almost the same distances across the five-speed steps, while MPV and SUV reported slightly lower values, up to 0.6 m less than FCR and RDS, Figure 3.6 (right). No predominant match with specific car parts was highlighted in any speed range, and no substantial evidence was found between the impact speed at which the OV hit the MC and the thrown distance of the dummy in lateral crashes.

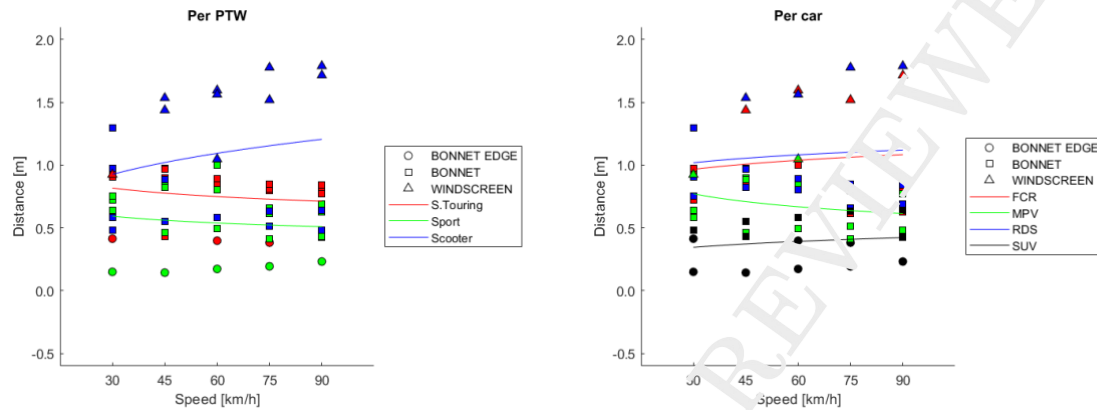


Figure 3.6 - Influence of speed in lateral crash per PTW (left) and per car (right). Every collision causing head contact was plotted in the scatter with a geometric symbol and a trendline was drawn over this data.

### 3.2.1 Influence of PTW

In this collision type, dummies ended their trajectories always with head contact on the OV's. The scooter maintained a significant ( $p\text{-value} < 0.01$ ) higher thrown distance ( $M=1.01$  m,  $SD=0.498$  m), Figure 3.7, hence, a higher percentage of contacts on the windscreen (45%), Figure 3.8, which the Chi-squared test attributed to the PTW style, Figure A.6 (c). Conversely, the sport-touring ( $M=0.84$  m,  $SD=0.213$  m) and the sport ( $M=0.62$  m,  $SD=0.262$  m) reported the shortest distances, not significantly different, turning into a comparable percentage of contacts on bonnet and bonnet edge. Each bar and boxplot counted for the same number of simulations ( $N=20$ ).

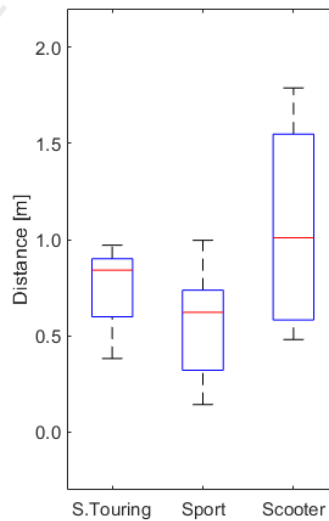


Figure 3.7 - Collision distance per PTW in lateral crashes.

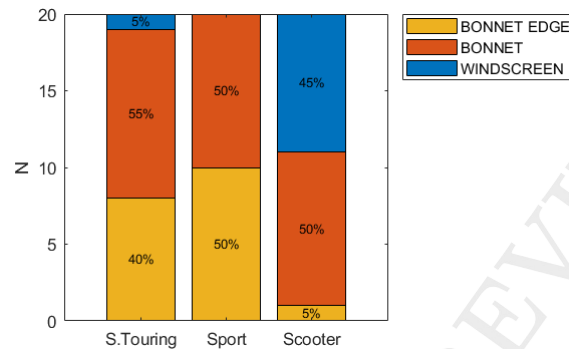


Figure 3.8 - Contact points per car parts across 15 TWs in lateral crashes.

### 3.2.2 Influence of car profile

A remarkable difference was noticed between car profiles: the SUV reported the shortest thrown distances among the four profiles ( $M=0.41$  m,  $SD=0.174$  m), significantly different from the others ( $p\text{-value} < 0.01$ ), Figure 3.9. Examining the contact points on the car profiles, it became evident that the SUV was the only profile with a substantial percentage of contacts (53%) occurring on the bonnet edge, which depended on the front-end design from the Chi-squared test, Figure A.6 (c); while no contacts were observed on the windscreen, Figure 3.10. In contrast, the remaining three profiles exhibited a higher percentage of contacts on the bonnet and a smaller portion, approximately one-quarter (lower for the MPV at 13%), on the windscreen. None of these three profiles showed an interaction with the bonnet edge in any simulation. Each bar and boxplot counted for the same number of simulations ( $N=15$ ).

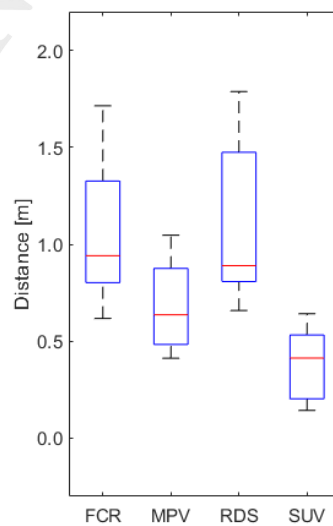


Figure 3.9 - Collision distance per car profile in lateral crashes.

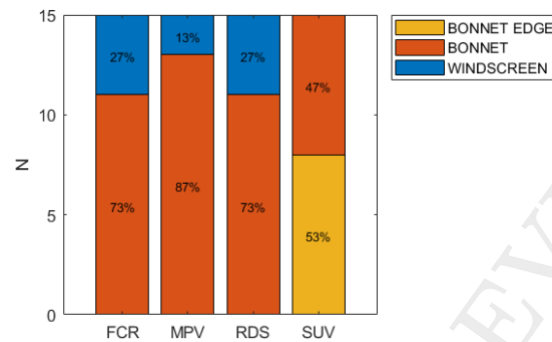


Figure 3.10 - Contact points per car parts across car profiles in lateral crashes.

## 4 Discussion

The frontal crash results showed that the rider's thrown distance depended on the MC speed, especially for sport and sport-touring PTWs. The contact on the windscreen happened only at speeds over 60 km/h, whereas the bonnet edge was prevalently hit at 30 and 45 km/h. As expected in frontal collisions, the bumper never hit the dummy, which collided solely with the PTW front wheel. Contact points on dummies and cars, indeed, depended on the trajectories developed during the collision, which in turn were determined by the PTW and car geometries. The data concerning rider-car contact points find evidence on a wide range of distinct trajectories, a phenomenon influenced by the inherent characteristics of PTWs, which highlights the unique dynamics at play during such collisions. Understanding these diverse trajectories is crucial for enhancing safety measures and accident prevention strategies in the context of PTW and car interactions. The rider on the scooter was prevalently restrained by the shielding of its vehicle, in agreement with other studies [8], with many no-contact instances against the OV and slight contacts on the bonnet after it turned around the PTW frontal headlamp. Only at the highest speeds was the dummy fully projected off the PTW, hitting the windscreen of the OV. Riders on the sport and sport-touring had more upward trajectories, maybe attributable to their different postures. The dummy on the sport-touring first hit the pelvis or lower limbs on the handlebars so that its flight was more vertical than forward, and it tended to overturn, with the head impacting on the OV in a rearward position, without any direct contact on the neck, as seen for cyclists in other studies, [9]. The dummy turned around the front of the MC, ending with head contact on the OV bonnet or even flying over the roof after a complete flip without any contact, in agreement with other studies [42]. Conversely, the sport PTW had a lower handlebar, promoting a free release of the dummy from the saddle with a high variance of end contacts and new body regions involved, such as the chest, in addition to the head and neck. From the point of view of cars, generally, as the height of the bonnet increased, there were more contacts on the head; conversely, with a lower bonnet height, there were more contacts on the chest, confirming the trend observed in pedestrians [43]. In the crashes against the OV with the highest bonnet, SUV, and MPV, the PTW pitch was lower, confirming that frontal structures may aim to control the energy transfer and prevent a rollover in frontals [44]. However, the dummy's motion was more upward than forward, which favored its rotation with direct head contact on the proximal part of the bonnet (short thrown distance). Conversely, FCR and RDS allowed extended thrown distances, and the riders hit the OV far away on the bonnet or directly on the windscreen. The RDS reported shorter distances and many no-contact instances, as the OV was more likely to move backward after the collision due

to its lighter mass; hence, using a reference system integral to the car, its distance median appeared lower, and its dependence on MC speed was higher. The no-contact distances were dominated primarily by two mechanisms: at low speed, dummies on sport and sport-touring were thrown over the PTW, falling to the ground without touching the OV and a slight rebound of both the vehicles; at high speed, riders could easily pass over the OVs (RDS and FCR) without touching it.

Different from frontal crashes, in laterals, the thrown distance did not show dependence on the OV impact speed, neither when it was analyzed per style of PTW nor type of OV. Conversely, the distance was greatly influenced by the PTW style since, after the first contact, the dummy lays down on the bonnet and develops its trajectory only if the lower limb is not restrained between the two vehicles. The fuel tank assumes a critical role in determining two potential outcomes: whether the dummy is trapped and experiences head contact with the bonnet or whether it remains free and subsequently strikes the windscreen with its head. Besides, the initial posture the dummy took on the PTWs determines its final distance: the more upright the dummy is, the further it is thrown after the crash. Thus, these combined elements correlate well with the finding that scooters are associated with the longest thrown distance in side impact scenarios. In addition, it is evident that OVs characterized by high profiles, such as MPVs and SUVs, played a significant role in confining the riders and preventing head contact with the windscreen. From this perspective, this study corroborates the findings that decreasing bumper height and bonnet length can increase head injury risk for riders [21,22] and pedestrian protection [45].

Although the OV profiles presented in this study are intended for trajectory assessment only, a certain level of riskiness can be inferred, considering that the car parts hit by riders have different stiffnesses and that the kinematics of the human body during the primary impact influence the severity of the injuries, at least for pedestrians, [46]. According to a study involving 153 PTW riders [42], the windscreen region (made by glass, wiper, and frame) resulted in the most dangerous, with an average AIS reported of 2.2, followed by the rear half of the bonnet (2.0), the bonnet leading edge (1.9), the bumper (1.7) and, eventually, the front half of the bonnet (1.2). Moreover, despite its low frequency (5%), cervical spine injuries were found to be extremely important, with an average AIS of 3.0, followed by injuries on the head (2.4, 60%), chest (2.2, 30%), and legs (1.9, 79%). The windscreen region was found likely to result in severe injuries not only for PTW riders [47] but also for head contact of pedestrians [9,48] and cyclists [9,16]. Based on the previous findings, RDS should represent a considerable threat for riders, given its high percentage of head contacts in lateral crashes and chest involvement in frontals, prevalently on the windscreen and rear bonnet. Conversely, the SUV may be more tolerant of riders, considering its contacts on the first half of the bonnet and their absence on the windscreen. Nevertheless, while certain vehicle variables, such as the inclination angle of the windscreen, appear to have no direct correlation with injuries [46], other studies propose that certain vehicles, such as SUVs, might possess bonnets that are even stiffer than windscreens found in compact cars [49]. However, since Otte's findings [42], many improvements interested the bonnet region, such as the pop-up bonnet ("Active Hood Lifting System") [50] and the pedestrian airbag, found effective also for cyclists [51]. Hence, assessing the influence of specific car components on the risk of injuries is a complex task [52]. It was emphasized that estimates of countermeasure efficacy cannot be based on the assumption that all injuries are solely caused by vehicle-related factors, but monitoring post-vehicle impact kinematics is crucial to address injuries during crashes completely [53].

This study showed that a higher bonnet height in frontal collisions was associated with an increased likelihood of head contact, while a lower height led to a higher chance of chest contact. In lateral impacts, the SUV effectively restrained riders with its bumper, avoiding contact with the windscreen. Statistical tests, such as the ANOVA and the Chi-squared tests, confirmed a significant correlation between the SUV front-end design and the thrown distances (or contact points). However, these tests also suggested that FCR, RDS, and MPV front-ends were not significantly different from a trajectory perspective, and, thus, they may be interchangeable for studies on car-to-PTW crashes. Differently, the PTW style significantly affected the outcome of frontal collisions: scooter riders rarely came into contact with the opposing vehicle; sport-touring motorcycles tended to have a higher likelihood of overturning with rearward head impact on the car; sport PTWs typically projected forward, increasing the likelihood of chest contacts. In lateral collisions, the presence of a conspicuous fuel tank on the PTW and the initial posture of the rider also played a significant role in determining the distance the rider was thrown: scooter riders were thrown further, often leading to head contact with the windscreen. These findings can serve as a valuable resource for future research aiming to design car profiles more forgiving towards PTW riders, ultimately enhancing their safety during crashes.



## A. Appendix

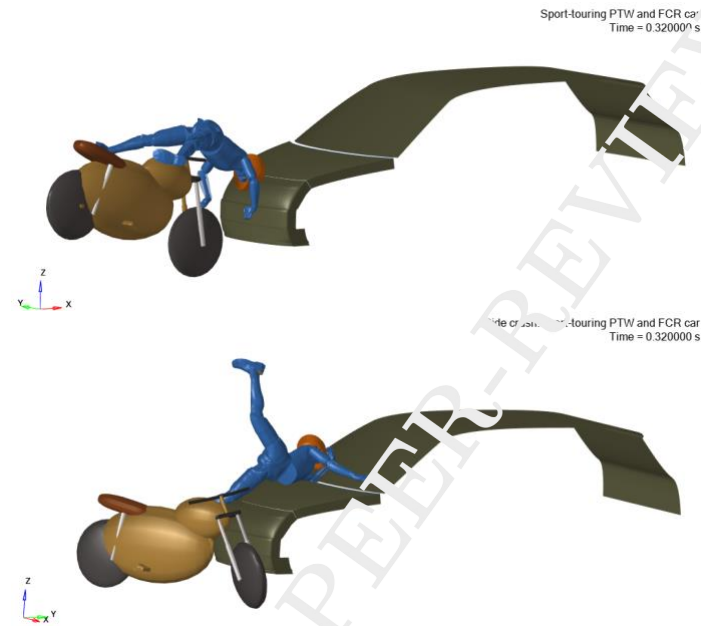


Figure A.1 - Frontal (upper) and side (lower) crashes reproduced in MADYMO.

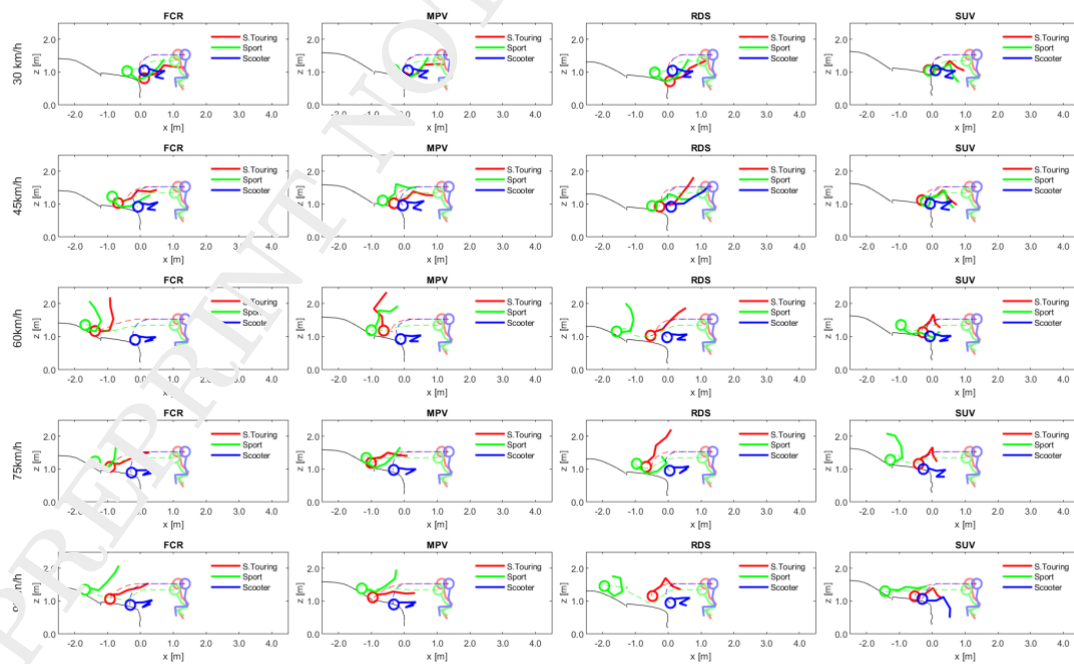


Figure A.2 - Overview of frontal collisions divided per OV across five-speed steps and grouped per PTW style.

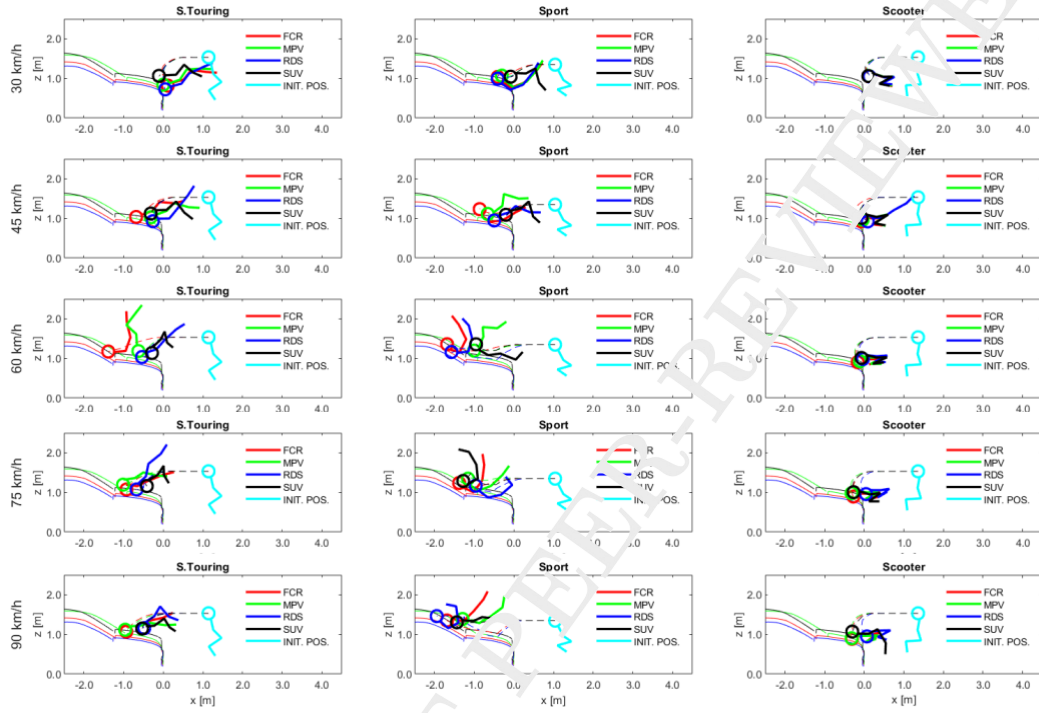


Figure A.3 - Overview of frontal collisions avoided per PTW across five-speed steps and grouped per OV style.

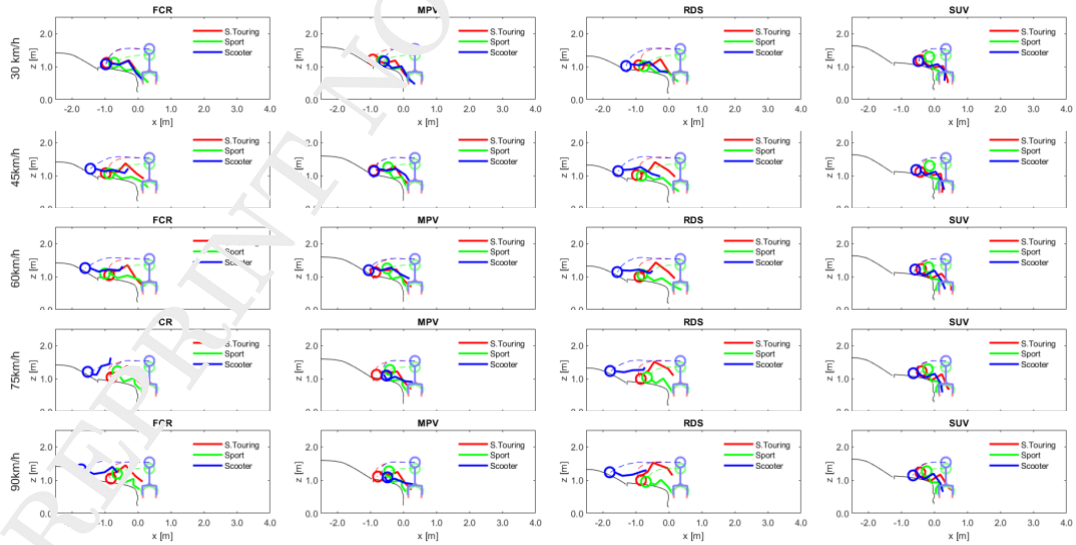


Figure A.4 - Overview of lateral collisions divided per OV across five-speed steps and grouped per PTW style.

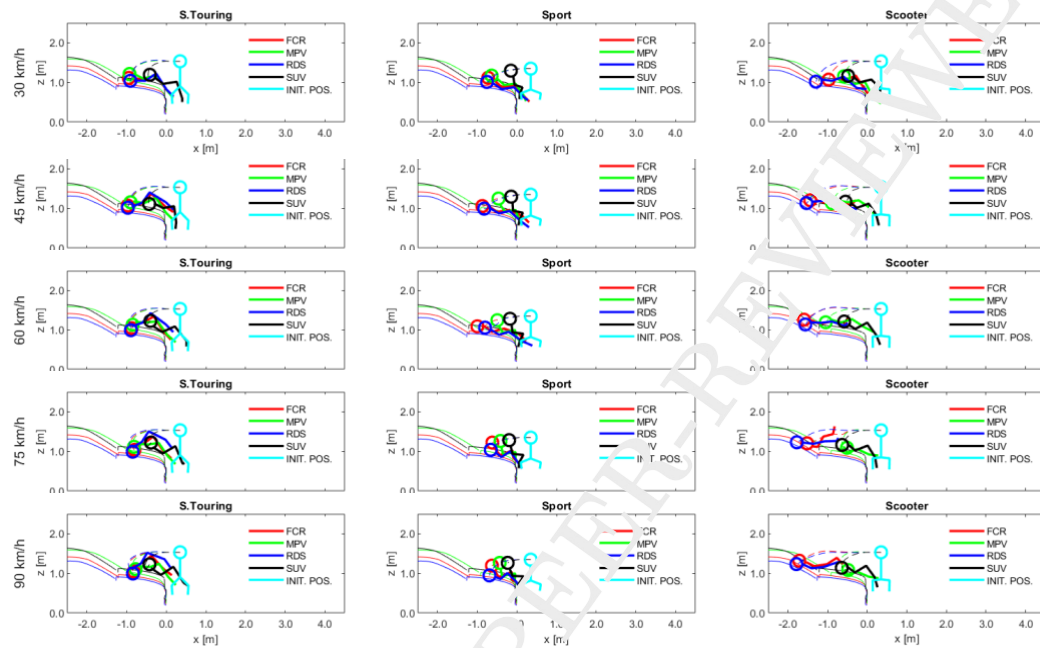


Figure A.5 - Overview of lateral collisions divided per PTW across five-speed steps and grouped per OV style.

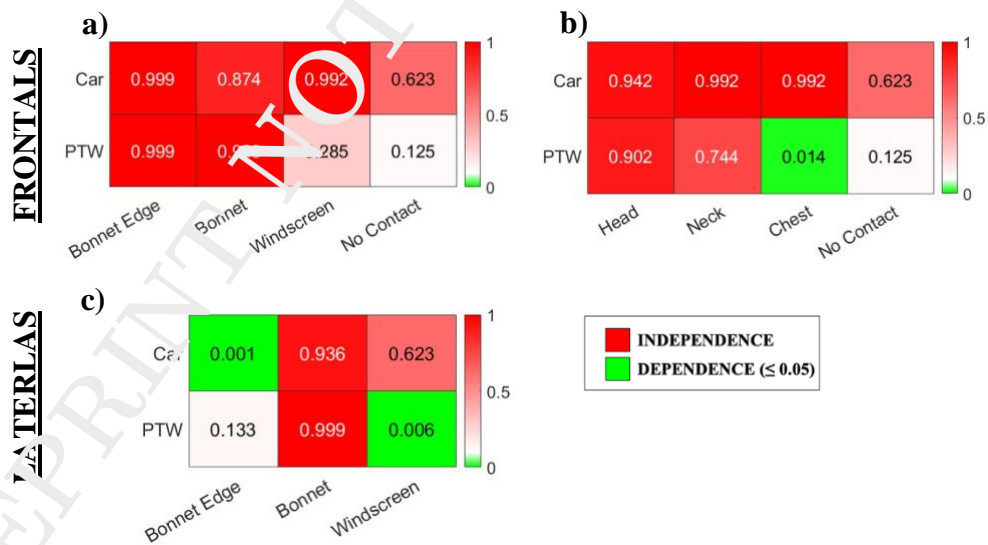


Figure A.6 - Chi-squared test at the 0.05 significance level for the independence of the variables (car parts and body regions) from the categorical groups (types of front-end and PTW) in head-on (first row) and side-on-head (second row) crashes.

## REFERENCES

- [1] Rizzi M 2016 *Towards a safe system approach to prevent health loss among motorcyclists* (Göteborg: Chalmers University of Technology)
- [2] Directorate General for Mobility and Transport 2023 *Road safety in the EU: fatalities below pre-pandemic levels but progress remains too slow*
- [3] Sloomans F 2023 *Facts and figures motorcyclists and mopeds*
- [4] European Commission 2018 *Communication from the commission to the European parliament, the council, the European economic and social committee and the committee of the regions* (Brussels)
- [5] Lubbe N, Wu Y and Jeppsson H 2022 Safe speeds: fatality and injury risks of pedestrians, cyclists, motorcyclists, and car drivers impacting the front of another passenger car as a function of closing speed and age *Traffic Safety Research* **2** 1–26
- [6] Simms C K and Wood D P 2006 Effects of pre-impact pedestrian position and motion on kinematics and injuries from vehicle and ground contact *International Journal of Crashworthiness* **11** 345–55
- [7] Li J, Fang S, Guo J, Fu T and Qiu M 2021 A Motorcyclist-Injury Severity Analysis: A Comparison of Single-, Two-, and Multi-Vehicle Crashes Using Latent Class Ordered Probit Model *Accid Anal Prev* **151**
- [8] Serre T and Llari M 2010 Numerical analysis of the impact between a PTW rider and a car in different accident configuration *IFMBE Proceedings* vol 31 pp 521–4
- [9] Nie J, Li G and Yang J 2015 A Study of Fatality Risk and Head Dynamic Response of Cyclist and Pedestrian Based on Passenger Car Accident Data Analysis and Simulations *Traffic Inj Prev* **16** 76–83
- [10] Mukherjee S, Chawla A, Mohan D, Singh M, Sakurai M and Tamura Y 2001 Motorcycle-car side impact simulation *Conference proceedings International Research Council on the Biomechanics of Injury, IRCOBI* (Isle of Man (UK): IRCOBI)
- [11] Serre T, Masson C, Perrin C, Martin J L, Moskal A and Llari M 2012 The motorcyclist impact against a light vehicle: Epidemiological, accidentological and biomechanical analysis *Accid Anal Prev* **49** 223–8
- [12] Chawla H, Koraca I and Savolainen P T 2019 Contrasting Crash- and Non-Crash-Involved Riders: Analysis of Data from the Motorcycle Crash Causation Study *Transp Res Rec* **2673** 122–31
- [13] Carrel J, Gidion F, Rizzi M and Lubbe N 2022 Do motorcyclist injuries depend on motorcycle and crash types? An analysis based on the German In-Depth Accident Study *International Motorcycle Conference (IFZ)*
- [14] Nelson P M 1979 Features of the Experimental Safety Motorcycle - ESM1 *International Technical Conference on Experimental Safety Vehicles (ESV)* (Paris (France): NHTSA)
- [15] Hurt H H Jr, Ouellet J V. and Thom D R 1981 *Motorcycle accident cause factors and identification of countermeasures* vol 1 (Los Angeles, California)
- [16] Peng Y, Chen Y, Yang J, Otte D and Willinger R 2012 A study of pedestrian and bicyclist exposure to head injury in passenger car collisions based on accident data and simulations *Saf Sci* **50** 1749–59
- [17] Van Rooij L, Bhalla K, Meissner M, Ivarsson J, Crandall J, Longhitano D, Takahashi Y, Dokko Y and Kikuchi Y 2003 Pedestrian crash reconstruction using multi-body modeling with geometrically detailed, validated vehicle models and advanced pedestrian

- injury criteria *International Technical Conference on the Enhanced Safety of Vehicles (ESV)*
- [18] Crocetta G, Piantini S, Pierini M and Simms C 2015 The influence of vehicle front-end design on pedestrian ground impact *Accid Anal Prev* **79** 56–69
  - [19] Li G, Lyons M, Wang B, Yang J, Otte D and Simms C 2017 The influence of passenger car front shape on pedestrian injury risk observed from German in-depth accident data *Accid Anal Prev* **101** 11–21
  - [20] Klug C, Feist F, Raffler M, Sinz W, Petit P, Ellway J and Van Ratingen M 2017 Development of a procedure to compare kinematics of human body models for pedestrian simulations *Conference proceedings International Research Council on the Biomechanics of Injury, IRCOBI* vol 2017-Septe (Antwerp (Belgium): IRCOBI) pp 508–30
  - [21] Xiao Z, Wang L, Mo F, Lv X and Yang C 2020 Influences of impact scenarios and vehicle front-end design on head injury risk of motorcyclist *Accid Anal Prev* **145** 1–11
  - [22] Xiao Z, Wang L, Zhang Y and Yang C 2022 A study on motorcyclist head responses during impact against front end of vehicle *International Journal of Crashworthiness* **27** 147–59
  - [23] Namiki H, Nakamura T and Iijima S 2005 A computer simulation for motorcycle rider injury evaluation in collision *International Technical Conference on the Enhanced Safety of Vehicles (ESV)* (Washington DC (USA): NHTSA)
  - [24] Barbani D, Baldanzini N and Pierini M 2014 Development and validation of an FE model for motorcycle-car crash test simulations *International Journal of Crashworthiness* **19** 244–62
  - [25] Yettram A L, Happier Smith J, Mo L S M, Macaulay M A and Chinn B P 1994 Computer simulation of motorcycle crash tests *International Technical Conference on the Enhanced Safety of Vehicles (ESV)* (Munich (Germany): NHTSA) pp 1227–40
  - [26] Grassi A, Barbani D, Baldanzini N, Barbieri R and Pierini M 2018 Belted Safety Jacket: a new concept in Powered Two-Wheeler passive safety *Procedia Structural Integrity* vol 8 (Elsevier B.V.) pp 573–93
  - [27] Xu S, Jin X, Luo C and Fu S 2021 Modeling method of rider-two-wheeler-road coupled system in two-wheeler traffic accident reconstructions *International Journal of Crashworthiness* 1–9
  - [28] Chén B O, Llari M, Afquir S, Martin J L, Bourdet N, Honoré V, Masson C and Arnoux P J 2019 Analysis of trunk impact conditions in motorcycle road accidents based on epidemiological, accidentological data and multi-body simulations *Accid Anal Prev* **127** 223–30
  - [29] Deguchi M 2005 Simulation of motorcycle-car collision *International Technical Conference on the Enhanced Safety of Vehicles (ESV)* (Washington (USA): NHTSA)
  - [30] Wang Q, Lou Y, Jin X, Kong L, Qin C and Hou X 2022 Reverse reconstruction of two-wheeled vehicle accident based on Facet vehicle model and hybrid human model *International Journal of Crashworthiness* **27** 661–76
  - [31] Himmetoglu S, Acar M, Bouazza-Marouf K and Taylor A J 2010 Whiplash protection by energy absorbing car-seat concepts *Biennial Conference on Engineering Systems Design and Analysis, ESDA2010* vol 3 (Istanbul, Turkey: ASME) pp 311–20
  - [32] Shokouhfar S 2017 *A Virtual Test Platform for Analyses of Rolling Tyres on Rigid and Deformable Terrains*

- [33] Shokouhfar S, Rakheja S and El-Gindy M 2015 Verification of the Port-Composite Approach for Modeling the Multi-Layered Structure of a Rolling Truck Tire *LS-DYNA Users Conference* (Würzburg (Germany): DYNAmore GmbH)
- [34] Wong J Y 1978 *Theory of Ground Vehicles* (John Wiley & Sons Inc.)
- [35] Perticone A, Barbani D and Baldanzini N 2023 Enhancing rider safety through Personal Protective Equipment: investigating the influence of Powered Two-Wheeler styles on the performance of the Belted Safety Jacket *Traffic Inj Prev* submitted
- [36] Perticone A, Barbani D and Baldanzini N 2023 Preliminary evaluation of a passive safety device concept for the protection of riders *International Journal of Crashworthiness*
- [37] Klug C and Ellway J 2021 *TB 024 - Pedestrian Human Model Certification*
- [38] Arunachalam M, Mondal C, Singh G and Karmakar S 2019 Motorcycle riding posture: A review *Measurement (Lond)* **134** 390–9
- [39] Smith T, Zellner J and Rogers M N 2006 A three dimensional analysis of riding posture on three different styles of motorcycle *International Motorcycle Safety Conference* (Long Beach (USA))
- [40] ISO 13232-6 2005 Motorcycles — Test and analysis procedures for research evaluation of rider crash protective devices fitted to motorcycles — Part 6: Full-scale impact-test procedures
- [41] Arunachalam M, Singh A K and Karmakar S 2021 Perceived comfortable posture and optimum riding position of Indian male motorcyclists for short-duration riding of standard motorcycles *Int J Ind Ergon* **83** 1–17
- [42] Otte D 1980 A Review of Different Kinematic Forms in Two-Wheel- Accidents-Their Influence on Effectiveness of Protective Measures *Stapp Car Crash Conference* (Troy (USA): SAE International) pp 561–605
- [43] Longhitano D, Henary B, Bhalla K, Ivarsson J and Crandall J 2005 Influence of Vehicle Body Type on Pedestrian Injury Distribution *SAE World Congress & Exhibition* (Detroit (USA): SAE International)
- [44] Maier S and Fehr J 2023 Accident simulations of a novel restraint safety concept for motorcyclists *International Technical Conference on Experimental Safety Vehicles (ESV)* (Yokohama (Japan): NHTSA)
- [45] Sankaranarayanan H, Göhlich D, Mukherjee S and Chawla A 2012 A bio-mechanics based methodology to optimize vehicle front profile for pedestrian safety *Proceedings of the 10th International Symposium on Biomechanics and Biomedical Engineering* pp 705–10
- [46] Otte D 2004 Use of Throw Distances of Pedestrians and Bicyclists as Part of a Scientific Accident Reconstruction Method *SAE World Congress & Exhibition* (Detroit (USA): SAE International) p 246
- [47] Piantini S, Pierini M, Delogu M, Baldanzini N, Franci A, Mangini M and Peris A 2016 Injury analysis of powered two-wheeler versus other-vehicle urban accidents *Conference proceedings International Research Council on the Biomechanics of Injury, IRCOBI* (Malaga (Spain): IRCOBI) pp 840–53
- [48] Otte D 1999 Severity and mechanism of head impacts in car to pedestrian accidents *Conference proceedings International Research Council on the Biomechanics of Injury, IRCOBI* (Sitges (Spain): IRCOBI)
- [49] Ballesteros M F, Dischinger P C and Langenberg P 2004 Pedestrian injuries and vehicle type in Maryland, 1995–1999 *Accid Anal Prev* **36** 73–81

- [50] Oh C, Kang Y and Kim W 2008 Assessing the safety benefits of an advanced vehicular technology for protecting pedestrians *Accid Anal Prev* **40** 935–42
- [51] Rodarius C, Mordaka J and Versmissen T 2008 *Bicycle safety in bicycle to car accidents*
- [52] Li G, Yang J and Simms C 2017 Safer passenger car front shapes for pedestrians: A computational approach to reduce overall pedestrian injury risk in realistic impact scenarios *Accid Anal Prev* **100** 97–110
- [53] Kendall R, Meissner M and Crandall J 2006 The Causes of Head Injury in Vehicle-Pedestrian Impacts: Comparing the Relative Danger of Vehicle and Road Surface *SAE World Congress & Exhibition* (Detroit (USA): SAE International)